Measuring the Leakage Current Module Characteristic of the HICANN Neuron Circuit

David Stöckel

July 31, 2014

Abstract

The HICANN wafer scale integrated circuits of Schemmel et al. [4] emulate the differential equations of the Adaptive Exponential Integrate-and-Fire neuron model [1]. The leakage term of this neuron model is implemented with an operational transconductance amplifier (OTA)— a voltage controlled current source. These OTAs are key circuits since they are used for many different terms of the AdEx emulation.

In this report the characteristic of the leakage OTA is measured in the transistor level simulation. The simulation includes the full two-denmem circuit to observe the influence of other components. These results are compared to data from hardware experiments.

Out of these measurements we obtain the leakage current characteristic. Especially the width of the linear range, the saturation regime and the corresponding uncertainties. We also find a mapping from the neuron parameters to simulated OTAs characteristic.

1. Introduction

The Adaptive Exponential Integrate-and-Fire Neuron Model [1] (AdEx) is an enhanced classical Integrate-and-Fire neuron model. Its dynamics are described by two differential equations. The first equation describes the dynamics of the membrane potential U. This membrane potential is coupled to an adaption current w.

$$C\frac{dU}{dt} = -g_L\left(U - E_L\right) + g_L\Delta_T \exp\left(\frac{U - U_T}{\Delta_T}\right) - w + I \tag{1}$$

$$\tau_w\frac{dw}{dt} = a\left(U - E_L\right) - w \tag{2}$$

The capacity C denotes the membrane capacity, g_L the leakage conductance, E_L the reversal potential, Δ_T the slope factor of the exponential rise and U_T the threshold potential. The current I is the external current input e.g. the synaptic input. In the

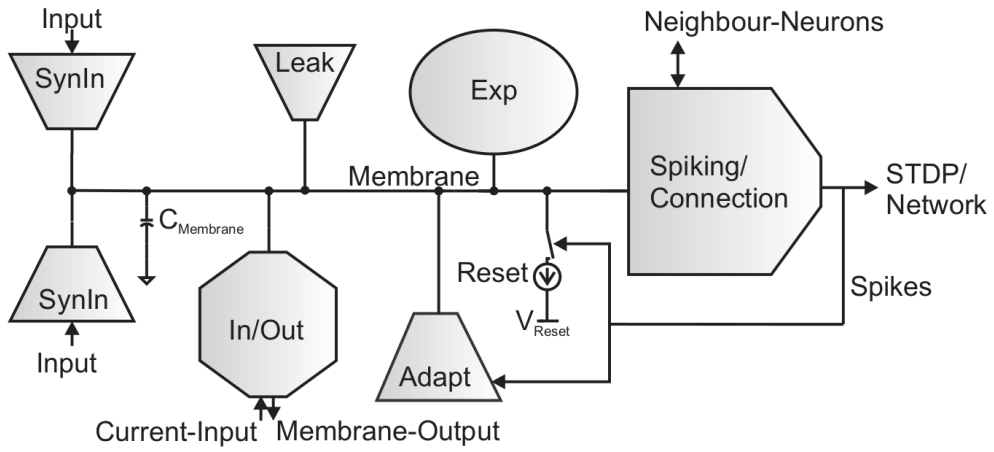

Figure 1: Simplified schematic of the AdEx implementation [3]. Each module represents a circuit that emulates one term of the AdEx differential equation.

second equation w is the adaption current, τ_w the time constant of the adaption current and a a coupling factor. If the membrane voltage U reaches the threshold voltage U_T the neuron spikes and the membrane voltage is set to U_{reset}.

The circuits on the HICANN chip [4] emulate these differential equations. The simplified schematic of the AdEx implementation taken from Millner et al. [3] is shown in figure 1. Each module is a circuit that represents a term of the AdEx differential equations.

The ion channels of the neuron—e.g. represented by the leakage term—are emulated by operational transconductance amplifiers (OTA). These are voltage controlled current sources. For an ideal OTA the output current is proportional to the difference of the input voltages. The slope of the output current as a function of the difference of the input voltages can be controlled by the current I_{gl}. For the OTA in the HICANN circuit the linear range depends this control current and is smaller than $\pm 400\,\mathrm{mV}$ [3]. The actual width of the linear range is discussed in detail in section 3.1 The application of the OTA in the leakage module is shown in figure 2. Within the linear range the OTA represents a conductance between the membrane voltage and the reversal potential. The reversal potential at which the output current is zero is set by E_L.

Since the OTA is a key circuit in the hardware neuron model this report discusses the measurement of the OTA's characteristic in the leakage module within the integrated circuit. On the hardware the only measurable value related to the leakage conductance is the time resolved membrane voltage. This implies that the information has to be extracted from the membrane voltage.

The measurements of the OTAs characteristic are made in the simulation. The proposed algorithm that extractes the characteristic is tested with data provided by Dominik Schmidt from the HICANN setup.

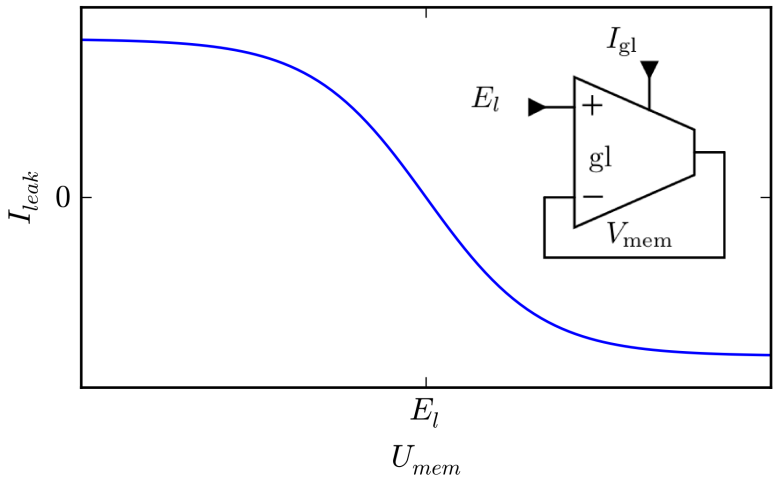

Figure 2: Schematic of the leakage module and the corresponding current–voltage characteristic.

2. Methods

On the HICANN chip no direct measurement of the leakage current is possible. It has to be derived from the cell membrane voltage, which can be measured using an analog readout circuit. This voltage U_{mem} is directly linked to the total sum of all currents I_j running from of the cell capacitor C.

$$\frac{dU_{mem}}{dt} = \frac{1}{C}\sum_j I_j \tag{3}$$

To obtain the leakage current from this equation the currents flowing through the other modules have to be known. This problem can be approached through choosing an appropriate measurement setup and compare it to the simulation. Following the AdEx model, the leakage current dominates when the cell membrane voltage is relaxing after a current input. In this report the focus will be on excitatory current inputs since the hardware offers only positive current inputs [4]. Therefore only membrane voltages larger than the reversal potential of the leakage term are accessible. This yields the characteristic $I(U)$ for negative currents.

2.1. Measurement sequence

After a relaxation time the neuron is stimulated with a short excitatory current input. It increases the membrane voltage from its resting potential U_r next to the threshold potential U_t. The current that represents the exponential term of the AdEx model is expected to grow exponentially when the membrane voltage is next to the threshold potential. It is therefore turned off. A further discussion of the exponential term is

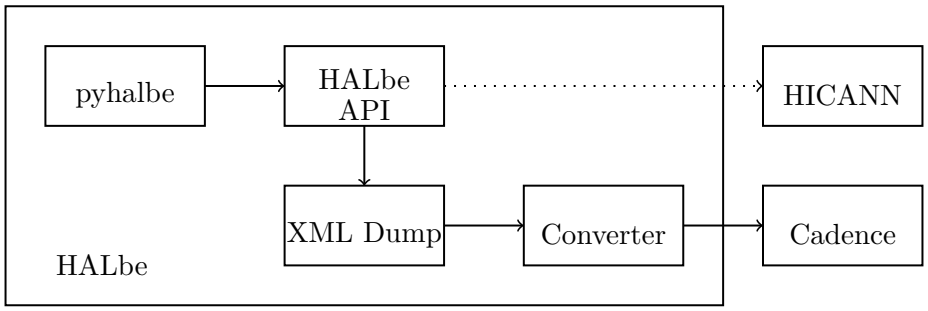

Figure 3: Sketch how the parameters are passed to the simulation software. The HALbe [2] library is used with the cadence backend. Another backend may be the HICANN wafer.

provided in the experiments section 3.2. The remaining currents through other modules are estimated with the simulation of this set up.

2.2. Simulation workflow

The neuron circuits are simulated with cadence on the transistor level. To configure the simulation all neuron parameters are passed to HALbe [2] with the pyhalbe API. These parameters include the neuron configuration and the stimulus. The halbe API is executed with a dump flag that toggles halbe to dump the configuration commands to an XML file. This XML file is then converted to a format that is readable by the simulation software. Figure 3 sketches how the simulation parameters are passed to the simulation software. The results of the simulation are written into a Json file. This Json file includes all currents and voltages on any component of the circuit.

2.3. Mathematical description

The simulation results provide all currents and voltages in the simulated circuit. Therefore we can directly plot the current-voltage characteristic of the leakage module. This measurements are taken to find an appropriate parameterization to describe the characteristic $I(U)$. As described in section 3.1 equation 4 fits the OTA characteristic of the simulation very good. Other tested parameterizations were a piecewise linear curve and a second order spline.

$$I(U) = a \log \left[\exp\left(-\frac{\alpha_I}{a}(U - U_s) \right) + \exp\left(-\frac{\alpha_{II}}{a}(U - U_s) \right) \right] - I_s \tag{4}$$

Figure 4 sketches this curve. The parameters of the equation are:

U_s Saturation voltage of the OTA

I_s Saturation current of the OTA

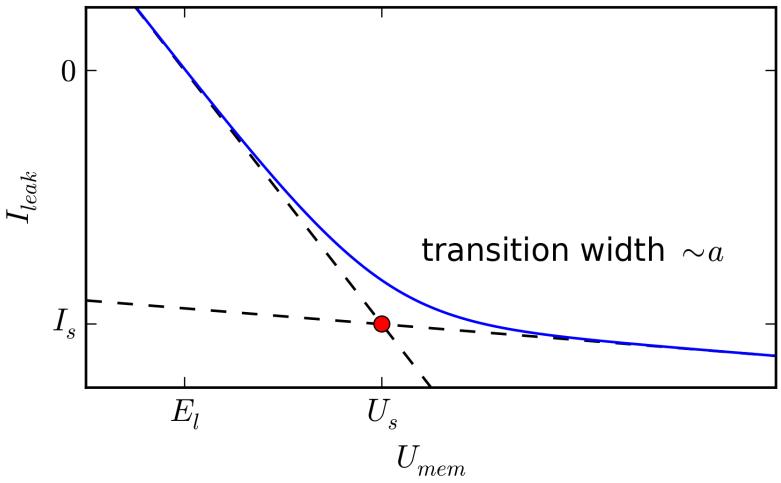

Figure 4: Sketch of the parameterization of the characteristic of the OTA. The slopes are given by α_I and α_{II}.

α_I Differential conductance of the OTA for $U << U_s$

α_{II} Differential conductance of the OTA for $U >> U_s$

a This parameter is related to the width of the transition from conductance α_I to α_{II}

For $a \to 0$ the function $I(U)$ is the maximum of two lines with slopes α_I and α_{II} and an intersection at (U_s, I_s). With larger a the transition from the first to the second line widens.

The differential conductance is the derivative of the current-voltage characteristic.

$$g(U) = -\frac{\partial I(U)}{\partial U} = \frac{\alpha_I e^{-\frac{\alpha_I}{a}(U-U_s)} + \alpha_{II} e^{-\frac{\alpha_{II}}{a}(U-U_s)}}{e^{-\frac{\alpha_I}{a}(U-U_s)} + e^{-\frac{\alpha_{II}}{a}(U-U_s)}} \tag{5}$$

The negative sign comes from the convention that positive currents are flowing onto the membrane capacitor. With the parameters one can calculate the width of the linear range. We define the linear range ΔU_{lin} as the range from E_l to the voltage where the ratio of the conductance relative to α_I is larger than a fixed parameter $0 < \delta < 1$. Within the linear range defined by the parameter δ there holds equation 6.

$$1 \leq \frac{g(E_l + \Delta_{lin})}{g(E_l)} \leq \delta \tag{6}$$

With the approximation that $E_l \approx U_s + \frac{I_s}{\alpha_I}$ we obtain a closed expression for the width of the linear range.

$$\Delta U_{lin}(\delta) = \frac{a}{\alpha_I - \alpha_{II}} \left[\log(1-\delta) - \log\left(\delta - \frac{\alpha_{II}}{\alpha_I}\right) \right] + \frac{I_s}{\alpha_I} \tag{7}$$

While equation 5 is invariant under the exchange of α_I and α_{II}, equation 7 only holds for $\alpha_I < \alpha_{II}$. This is due to the approximation of E_l which is only valid for α_I larger than α_{II}.

Assuming that only the leakage current I is flowing out of the membrane capacitor C the time dependence of the membrane voltage is given by the following differential equation.

$$\frac{dU}{dt} = \frac{I(U)}{C} \tag{8}$$

$$U(t) = U_p + \frac{1}{C}\int_{t_0}^{t} I(U(t'))dt' \tag{9}$$

Equation 9 is the equation that is used for solving equation 8 numerically with the boundary condition $U(t_0) = U_p$. This equation is fitted to the membrane voltages measured in the simulation and to the data provided from the HICANN setup. There are therefore 6 free parameters. 5 parameters describing the OTA's characteristic and one parameter—U_p—as a boundary condition of the integral. If this function fits to the data we have extracted the parameters, especially α_I for the leakage current.

Within the linear range of the OTA, which is in the range $E_l < U < U_s$, the membrane voltage follows an exponential decay towards the reversal potential E_l if there are no other currents except the leakage current.

$$U(t) = (U_p - E_l)\exp\left(-\frac{t - t_0}{\tau}\right) + E_l \tag{10}$$

The time t_0 and the voltage U_p are the initial condition of this exponential decay. From the parameter α_I we can derive the time constant τ of this process.

$$\tau = \frac{C}{\alpha_I} \tag{11}$$

3. Experiments and Results

3.1. Simulation

The simulation is executed with different OTA control currents. The parameter I_{gl}^{param} is variied from 200 nA to 2400 nA in steps of 200 nA. This current is scaled down with a current mirror that has three different settings. This current mirror is included in the simulation as well. In its default configuration the current is scaled down with a factor designed to be 3. The factor measured in the simulation is $2.75^{+0.10}_{-0.22}$. Figure 5 shows the membrane voltage for the simulation run with $I_{gl}^{param} = 400\,\text{nA}$. The full parameter set used in the simulation is listed in table 3. After a time of 5 µs there is an excitatory current input of 1.2 mA for 0.55 µs to the membrane capacitor. The membrane voltage rises within this time from 0.60 V to $\approx$ 1.10 V. After this current input the voltage of the capacitor falls back to its resting potential of 600 mV which is equivalent to the reversal potential E_l of the leakage current. As expected this relaxation is driven by the leakage module. According to I_{gl} the leakage current at the membrane's peak voltage is

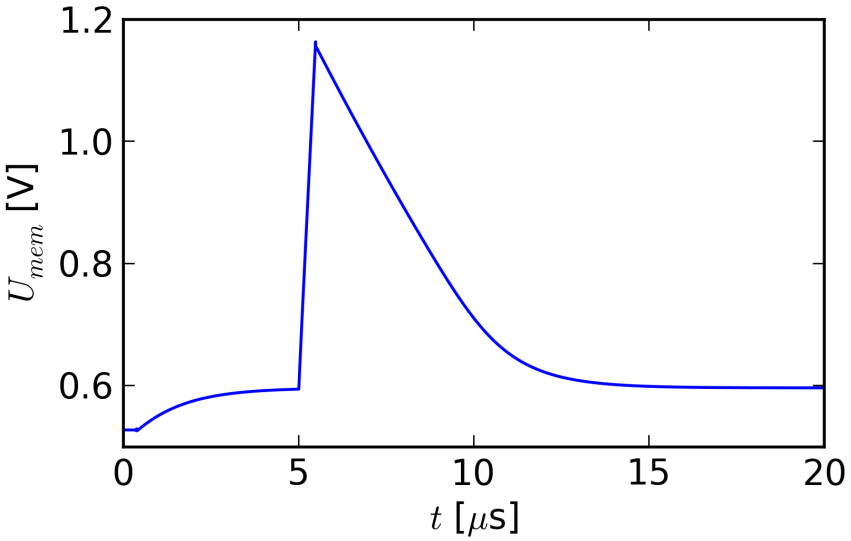

Figure 5: Voltage of the membrane capacitor during one simulation run with $I_{gl}^{param} = 400\,\mathrm{nA}$.

between 115 nA and 953 nA. There is also a current running through the excitatory and inhibitory synaptic input with a total sum smaller than 38 nA. Figure 10 in the appendix shows this currents through the synaptic inputs for different membrane voltages. The sum of the synaptic input currents goes to zero as the membrane voltage goes to the reversal potential. The currents running through the other modules are each smaller than 1 nA.

While the OTA's characteristic can directly be extracted from the simulation results, the total neuron characteristic $I(U_{mem})$ has to be calculated with equation 12. The current I is the sum of all currents, not only the leakage current.

$$I(U_{mem}) = C \cdot \frac{dU_{mem}}{dt} \tag{12}$$

The voltage as a function of time returned by the simulation is smooth enough to be calculated numerically by dividing the differences of the voltage array by the differences in the time array. There is no noise in the membrane voltage of the simulation.

There were different parameterizations tested for the measured OTA U-I characteristic. Equation 4 fits the OTA characteristic very good. Other tested curves are a quadratic spline or a piecewise linear function. The curve was fitted with the membrane voltage as a function of time, which means that $U_{mem}(t)$ was fitted with the numerically solved differential equation 9. The absolute residuals vary within $\pm 124\,\mu\mathrm{V}$. As described before there is no noise in the voltage returned by the simulation. The numerical calculation precision of 0.11 fV is smaller by four orders of magnitude. Therefore all residuals are systematic errors. Figure 6 shows the fitted voltage for $I_{gl} = 152\,\mathrm{nA}$ and the errors relative to the voltage.

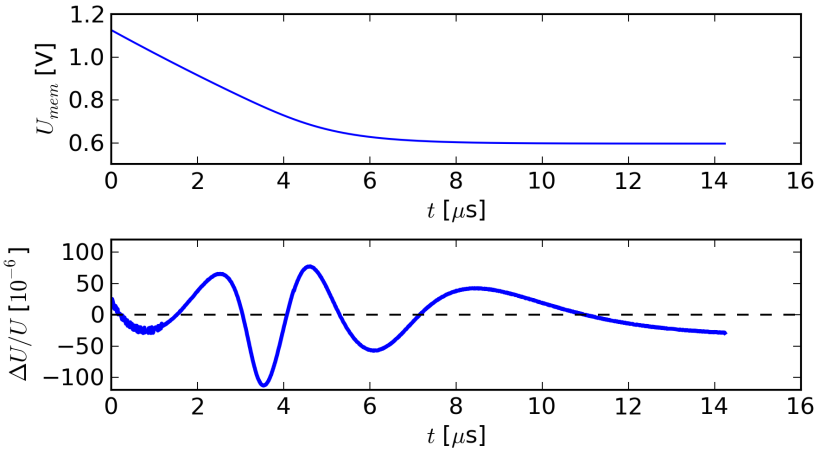

Figure 6: The upper plot shows the fitted voltage as a function of time returned by the simulation for $I_{gl} = 152\,\text{nA}$. The residuals of the curve fit with equation 9 are shown below. They are normalized to the corresponding membrane voltage. In the upper plot the measured curve isn't drawn since it is indistinguishable on the drawn voltage scale.

The fit parameters for the different control currents are plotted in the appendix C as a function of I_{gl}^{param}. Since the curve was fitted to the membrane voltage the fit parameters describe the $I(U_{mem})$ dependence and not the isolated OTA characteristic. The conductances for different control currents derived by the curve fit are shown in figures 7.

There are large non diagonal elements in the correlation matrix of the fit parameters, therefore the fit might easily become unstable. These large correlations have to be taken into account when calculating uncertainties of the current voltage-characteristic (compare section 3.3.1). Matrix 13 is the correlation matrix for $I_{gl} = 250\,\text{nA}$.

$$\begin{array}{c} \\ \alpha_I \\ \alpha_{II} \\ I_s \\ U_s \\ a \\ U_p \end{array} \begin{array}{c} \begin{array}{cccccc} \alpha_I & \alpha_{II} & I_s & U_s & a & U_p \end{array} \\ \begin{pmatrix} 1.0 & & & & & \\ -0.67 & 1.0 & & & & \\ -0.69 & 0.99 & 1.0 & & & \\ -0.90 & 0.29 & 0.30 & 1.0 & & \\ 0.96 & -0.83 & -0.86 & -0.75 & 1.0 & \\ -0.28 & 0.68 & 0.59 & 0.01 & -0.40 & 1.0 \end{pmatrix} \end{array} \tag{13}$$

The correlation matrix gives a measure of the correlation of two fit parameters. Let $x = (\alpha_I, \alpha_{II}, I_s, U_s, a, U_p)$ be the vector of the parameter set. An entry in the correlation matrix at position (i, j) is the expectation value $E(x_i x_j) - E(x_i)E(x_j)$ normalized to the error $\Delta x_i \Delta x_j$. Two variables coding the same information have a correlation of 1.0 or -1.0.

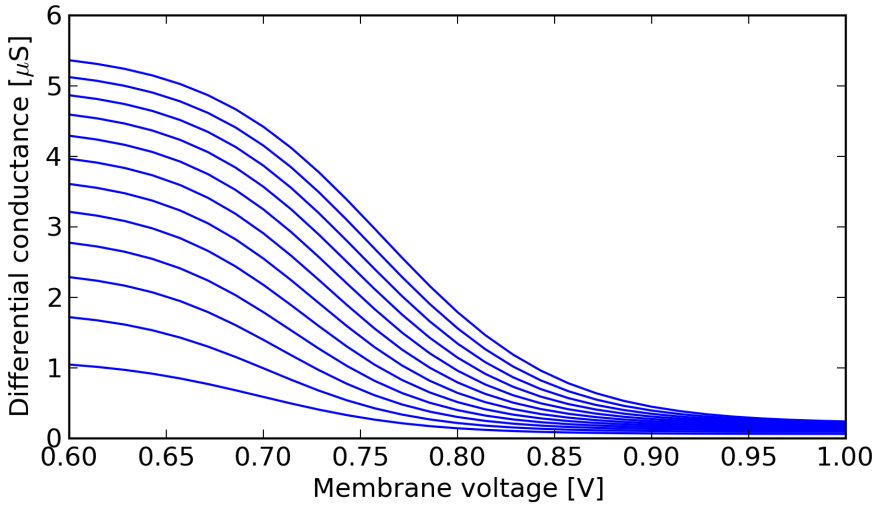

Figure 7: Differential conductances for different control currents of the OTA. The control current I_{gl} is varied from 79 nA to 841 nA. This corresponds to parameter I_{gl}^{param} is varied from 200 nA to 2400 nA in steps of 200 nA. The largest control current leads to the largest conductance.

3.2. Disabling the Exponential Leakage Current

As described in section 2 the module representing the exponential current is supposed to be turned off. The operational amplifier of the circuit representing the exponential term can be disabled by setting $I_{bexp} = 0\,\text{nA}$. It was found that disabling the operational amplifier of the exponential circuit is not sufficient.

With the configuration of the exponential term shown in table 1 a current of $I_{exp} = 250\,\text{nA}$ is running onto the cell membrane in its equilibrium state. The cell membrane

parameter	value	comment
V_{bexp}	1042 nA	control current for V_{exp} buffer
I_{bexp}	0 nA	control current for the exponential term OP
V_{exp}	536 mV	threshold voltage for the exponential current
I_{rexp}	750 nA	strength of exponential term

Table 1: Parameter set concerning the exponential term, leading to a large current flowing onto the cell membrane in its equilibrium state. All other parameters in the simulation run are the ones listed in table 3. The reason for this current is that a current $V_{bexp} = 1042\,\text{nA}$ disables the unity gain buffer of V_{exp}. It is enabled with $V_{bexp} = 0\,\text{nA}$.

voltage is then 717 mV in its equilibrium instead of the expected resting potential which

should be equal to the parameter $E_l = 600\,\text{mV}$. The current I_{exp} is compensated by the leakage current.

When the cell's membrane voltage is higher than 0.900 mV the current I_{exp} is zero. Below this threshold the exponential current increases rapidly and saturates at a membrane voltage of 770 mV with a value of 250 nA.

The experiment described above was accidentially taken with a disabled unity gain buffer for V_{exp}. A unity gain buffer is an amplifier with a amplification factor of one. They are needed for the parameters V_{exp} and I_{exp} since multiple neurons share the samce digital to analog converter. The voltage controlled by the V_{exp} buffer was 1120 mV. This high voltage after the buffer explains this large current running onto the membrane capacitor when the membrane voltage drops below 900 mV.

3.2.1. Tested Parameter Sets

To avoid such an unexpected current running through the exponential term in the future, different parameter sets where tested. Three variables are measured for each parameter set. The current running from the exponential term module onto the membrane capacitor, the membrane voltage and the voltage controlled by the input buffer.

The simulation without the stimulus was executed for those different parameter sets listed in table 5. The voltages and currents were measured after a relaxation time $> 10\,\text{ms}$. Appendix D contains a summary of the tested parameter sets and a short description of the parameters.

With the activated input buffer for V_{exp} no unexpected currents ran onto the cell membrane. Therefore in future experiments one should always enable the unity gain buffer of the voltage V_{exp} even if the exponential term is supposed to be turned off. It is not sufficient to disable the OP of the exponential term circuit.

3.3. Hardware

The parameterization in equation 4 for the current voltage characteristic was derived from the simulation phenomenologically. Data of the same stimulation process as described in methods section is provided for 63 neurons on the HICANN wafer by Dominik Schmidt. The membrane voltage is sampled with a frequenzy of 96 MHz. Those membrane voltages are averaged over multiple runs of the stimulation process for each neuron.

Since only the relaxation process is of interest, the $U(t)$ measurements are cut 50 time steps after the maximum voltage. This is a very simple method but proofed to be successful in most cases. It fails for 9 out of the 63 neurons. In this 9 cases the cutted data doesn't show the relaxation process, therefore those were removed from the sample. There are 3 neurons where the averaging process failed since the data wasn't triggered correctly. For one neuron the relaxation process wasn't centered in the trace. They are removed from the neuron data samples as well. Figure 17 shows such a bad neuron. There are 50 $U(t)$ samples left for different neurons.

To each of these neurons the curve 9 is fitted with the 6 free parameters. As described in the simulation section (3.1) the correlation matrix for the simulation fit shows large

category	number of neurons
statistical error	10
systematic periodic error	27
systematic error	12

Table 2: Number of neurons in the different categories

non diagonal elements, e.g., a large correlation between α_{II} and I_s. It turned out that the fit didn't converge for many neurons if not either α_{II} or a was fixed[1]. α_{II} was therefore set to 72.8 nS. This is the differential conductance extracted from the simulation results at $I_{gl}^{param} = 250\,\text{nA}$. All fits of the 50 neurons converged for fixed α_{II} within 10000 iterations. The membrane voltage noise was measured for each neuron and taken as its voltage uncertainty. The fit parameters show very large uncertainties for some neurons. Those high uncertainties are the result of the large correlation between the parameters a and I_s. This also results in large fit times for some measurements. The fit times with a fixed parameter α_{II} are $0.6^{+8.0}_{-0.5}$s There is a very large deviation in the positive direction of the fit time. The fit time of the Levenberg-Marquardt algorithm implemented in [5] was taken with an 64-bit quad core processor running at 800 MHz.

Looking at the residuals of the fits, there are three different error patterns. The error patterns are in the following referenced as 'statistical error', 'periodic systematic error' and 'systematic error':

statistical error The residuals are spreading symmetrically in the $\pm 3\sigma$ range. See figure 18.

periodic systematic error The residuals vary periodically. The frequency is much higher than the time constant. See figure 20.

systematic error The residuals show a systematic deviation from the fitted curve. See figure 22.

In the section E there are graphs shown for fits of each of those groups. Table 2 shows the number of neurons in those categories.

The parameter a that describes the transition width from conductance α_I to α_{II} has a very large uncertainty for all neurons. The mean value of $a = 50\,\text{nA}$ is within the uncertainty range of all the neuron's fit values for a and is set fixed. This is done to minimize large correlations between the free fit parameters. With a fixed the fitting algorithm converges much faster as expected. The uncertainties for the other parameters shrink significantly as well. This is due to the eliminating the large cross correlations with fixing one of the correlated values. The fit times with fixed α_{II} and a are $0.083^{+0.025}_{-0.014}$s on the same machine. There are now 4 free parameters left—α_I, U_s, I_s, U_p—of which 3 describe the OTA's characteristic. The parameters of the fitted curves for the 50 neurons are shown in figure 8.

[1] The data was fitted with the Levenberg-Marquardt algorithm implemented in numpy [5]. For the

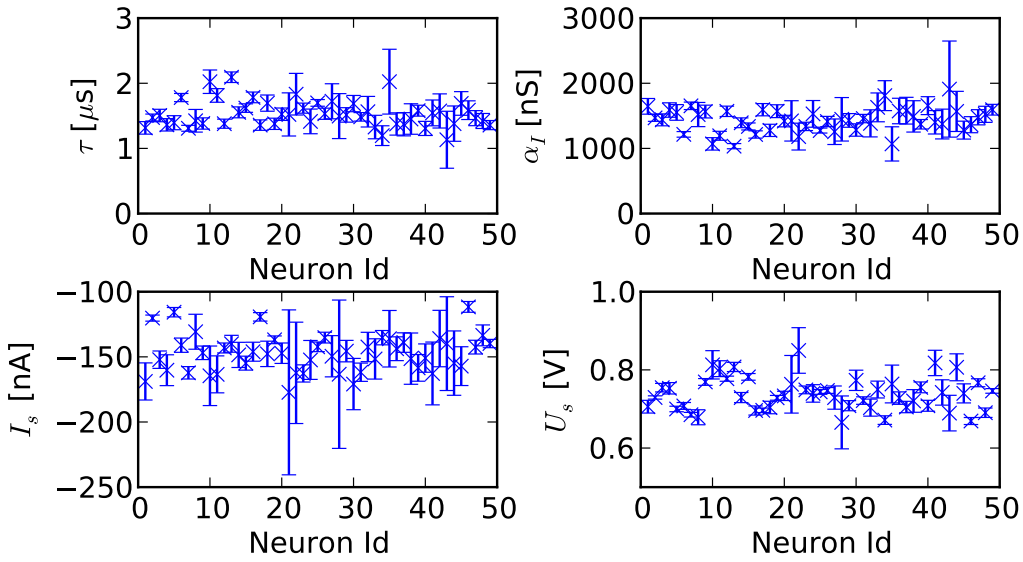

Figure 8: The fit parameters for the hardware neurons, excluding the bad neurons. The time constant τ_I is derived from parameter α_I—see section 2.

3.3.1. Extracted Characteristics

The parameters returned by the fit algorithm describe the $I(U)$ characteristic of the OTA of the leakage module. The uncertainty of the characteristic can be calculated from the parameter uncertainties as well. Since the covariances are large, relative to the parameter uncertainties, they have to be taken into account. At a voltage U and for a given parameter set x the uncertainty of the current $I(U;x)$ is calculated with equation 14.

$$\Delta I = \sqrt{\sum_{i,j} \left(\frac{\partial I}{\partial x_i}\right) \left(\frac{\partial I}{\partial x_j}\right) \Delta(x_i x_j)} \tag{14}$$

$\Delta(x_i x_j)$ denotes the covariance between parameter x_i and x_j. For $i = j$ this is the variance of parameter x_i. The sum is over $i, j \in \{\alpha_I, U_s, I_s\}$. The cross correlation terms are therefore summarized twice each.

In the appendix E figure 19, 21, 23 and 25 show the extracted characteristics and the uncertainties for specific neurons. In the same graphs there are also shown the measured data points. The currents are calculated with $I = C\frac{\Delta U}{\Delta t}$. One point in the graph is the average over 25 values. The error bars are the error of the average—which is the standard deviation of the 25 values divided by the square root of the count of samples minus one. It needs to be noted that 25 samples represent a time difference shorter

desired output errors the default values were taken. The number of maximum iterations is set to 10000.

that the typical period of the periodic systematic errors seen with many neurons, e.g. figure 20.

It can be seen why the calculation with a free slope parameter α_{II} failed for many neurons. There are not enough data points for high voltages which could give a precise curve shape in the saturation regime. An example for a large uncertainty for high voltages due to few data points at large membrane voltages is shown in figure 9.

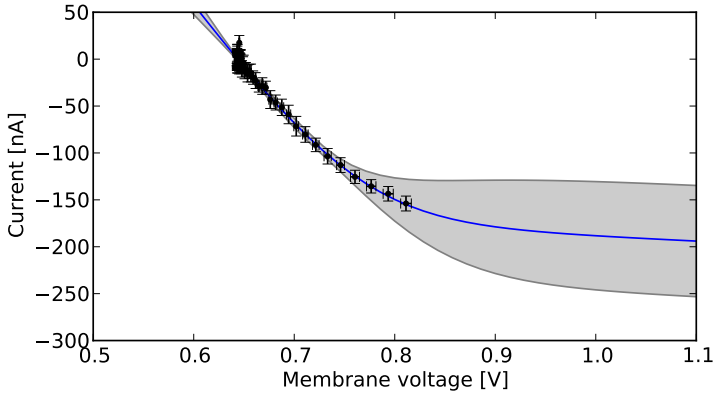

Figure 9: The $I(U)$ characteristic for a neuron with few data points for high voltages. The saturation current can't be estimated precisely.

4. Discussion

The fit of the proposed parameterization 4 extracts the leakage current module characteristic of a simulated neuron circuit. It yields intuitively accessible parameters of the leakage module. This includes the differential conductance in the linear and in the saturation regime. Parameters describing the transition from the linear to the saturation regime are the saturation voltage, the saturation current and the transition width. The measured characteristic is biased by leakage currents through other circuits connected to the membrane capacitor.

For the conductance at membrane voltages next to E_l we find the calibration curve 15.

$$\alpha_I = \left[\left(\frac{I_{gl}^{param}}{1.286 \times 10^{-5}\,\mathrm{nA}} \right)^{0.4615} - 1027 \right] \times 1\,\mathrm{nS} \tag{15}$$

This characteristic was also extracted from membrane voltage data of neurons on the HICANN wafer. For the 53 data samples the parameters of the characteristic were extracted if the conductance in the saturation regime was set to a fixed value. Otherwise the Levenberg-Marquardt algorithm used for the fit wouldn't converge. The fit time can be improved significantly by setting the transition width fixed as well. The processing for one neuron measurement takes $0.083^{+0.03}_{-0.01}$s for 4 free parameters, and $0.6^{+8.0}_{-0.5}$s for 5

free parameters. The efficiency of the suggested workflow regarding computational cost and small uncertainties strongly depends on the coverage of the saturation regime in the data sample.

To make this calibration workflow practicable the data has to be filtered automatically. In this report the bad traces were sorted out by hand. Data samples that don't cover the saturation regime need to be filtered as well. As another point the trigger of the falling edge of the membrane voltage in the data samples has to be improved. In this report 9 traces out of 63 were triggered wrong. With this improvements the proposed parameterization may be used in the hardware calibration process to yield a detailed view on the neuron's leakage circuit.

References

[1] W. Gerstner and R. Brette. Adaptive exponential integrate-and-fire model. 4(6):8427, 2009. revision #90944.

[2] Electronic Vision(s) Group. Hmf halbe (hal backend), 2014.

[3] Sebastian Millner, Andreas Grübl, Karlheinz Meier, Johannes Schemmel, and Marc olivier Schwartz. A vlsi implementation of the adaptive exponential integrate-and-fire neuron model. In J.D. Lafferty, C.K.I. Williams, J. Shawe-Taylor, R.S. Zemel, and A. Culotta, editors, *Advances in Neural Information Processing Systems 23*, pages 1642–1650. Curran Associates, Inc., 2010.

[4] Johannes Schemmel, Andreas Grübl, and Sebastian Millner. Specification of the hicann microchip. *FACETS project internal documentation*, 2010.

[5] Stéfan van der Walt, S. Chris Colbert, and Gaël Varoquaux. The numpy array: A structure for efficient numerical computation. *Computing in Science & Engineering*, 13(2):22–30, 2011.

A. Full Simulation Parameter Set

parameter	value	comment
E_l	600 mV	the reversal potential of the leakage current
E_{syni}	500 mV	
E_{synx}	700 mV	
I_{bexp}	0 nA	control current of the exponential term OP. Zero is off
I_{convi}	2500 nA	bias current for synaptic input
I_{convx}	2500 nA	bias current for synaptic input
I_{fire}	0 nA	adaptation term b
$I_{gladapt}$	0 nA	adaptation term
I_{gl}^{param}	$200 - 2400$ nA	corresponds to a control current of the OTA of $79 - 841$ nA
I_{intbbi}	2000 nA	integrator bias in synapse
I_{intbbx}	2000 nA	integrator bias in synapse
I_{pl}	2000 nA	
I_{radapt}	2500 nA	
I_{rexp}	0 nA	control current of R_{exp}
$I_{spikeamp}$	2000 nA	
V_{exp}	536 mV	exponential term threshold current
V_{syni}	1000 mV	technical parameter that drives the integrator
V_{syntci}	1375 mV	inhibitory synapse input
V_{syntcx}	1375 mV	excitatory synapse input
V_{synx}	1000 mV	technical parameter that drives the integrator
V_t	1000 mV	threshold potential
V_{bout}	750 mV	
V_{bexp}	1042 nA	control current for the unity gain buffer of V_{exp}. Zero is on
fast I_{gl}	False	
slow I_{gl}	False	
bigcap	True	

Table 3: Base parameters used in the simulation and on the hardware measurements.

B. Currents Through the Synaptic Input

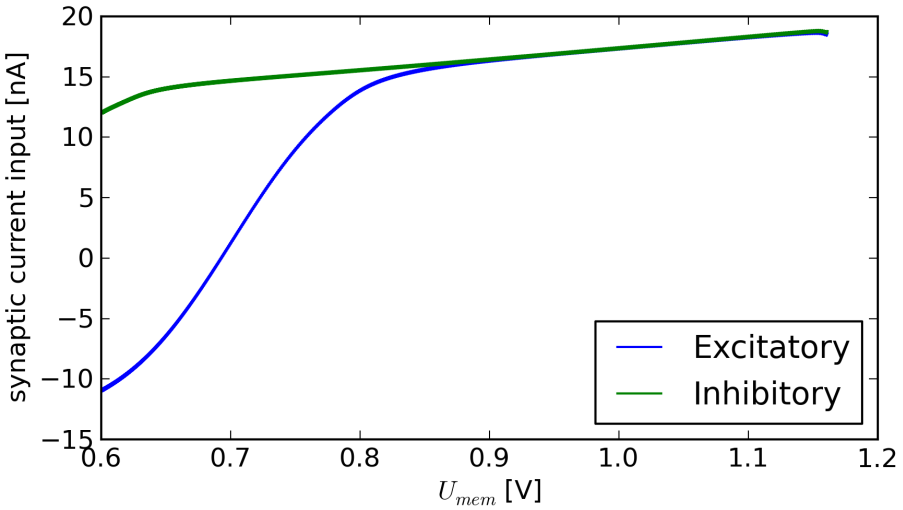

Figure 10: Currents running through the excitatory and inhibitory synaptic input at different membrane voltages.

C. Simulation Fit Results

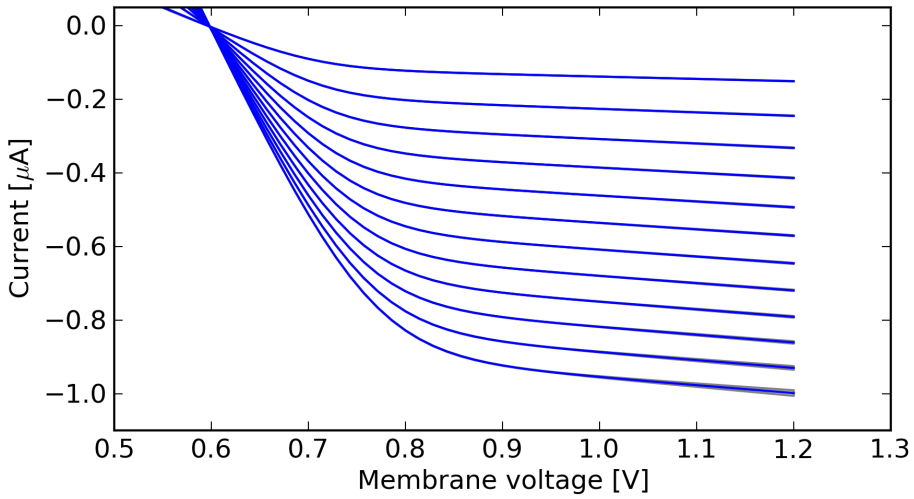

Figure 11: Fitted characteristics. The control current I_{gl} is varied from 79 nA to 841 nA. This corresponds to parameter I_{gl}^{param} varied from 200 nA to 2400 nA in steps of 200 nA. The uncertainties — only visible for the largest control current — are calculated with the error propagation considering also the correlation coefficients described in section 3.3.1.

parameter	**calculation**
Conductance α_I	$\left[\left(\frac{I_{gl}^{param}}{1.286 \times 10^{-5}\,\mathrm{nA}}\right)^{0.4615} - 1027\right] \times 1\,\mathrm{nS}$
Conductance α_{II}	$\left[\left(\frac{I_{gl}^{param}}{5.722 \times 10^{-5}\,\mathrm{nA}}\right)^{0.3264} - 74.22\right] \times 1\,\mathrm{nS}$
Transition width a	$\left[\left(\frac{I_{gl}^{param}}{4.902\,\mathrm{nA}}\right)^{0.8694} + 19.20\right] \times 1\,\mathrm{nA}$
Saturation current I_s	$\left[-\left(\frac{I_{gl}^{param}}{1.674\,\mathrm{nA}}\right)^{0.9311} - 33.37\right] \times 1\,\mathrm{nA}$
Saturation voltage U_s	$\left[\left(\frac{I_{gl}^{param}}{4.048 \times 10^{4}\,\mathrm{nA}}\right)^{0.9315} + 0.6892\right] \times 1\,\mathrm{V}$

Table 4: Calculation of the fit parameter as a function of I_{gl}^{param}. These functions are drawn in the following corresponding plots with a blue line.

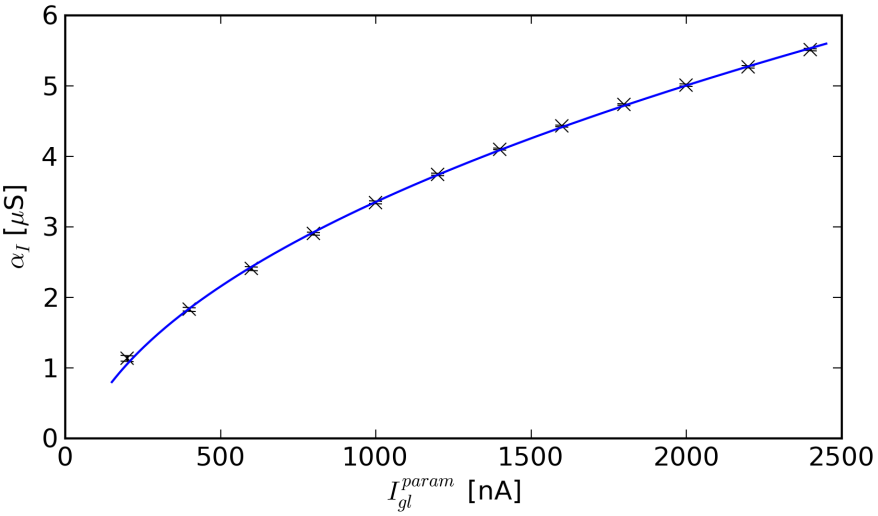

Figure 12: Differential conductance α_I for membrane voltages next to the reversal potential as a function of the OTA control current. The parameterization of the blue line is listed in table 4.

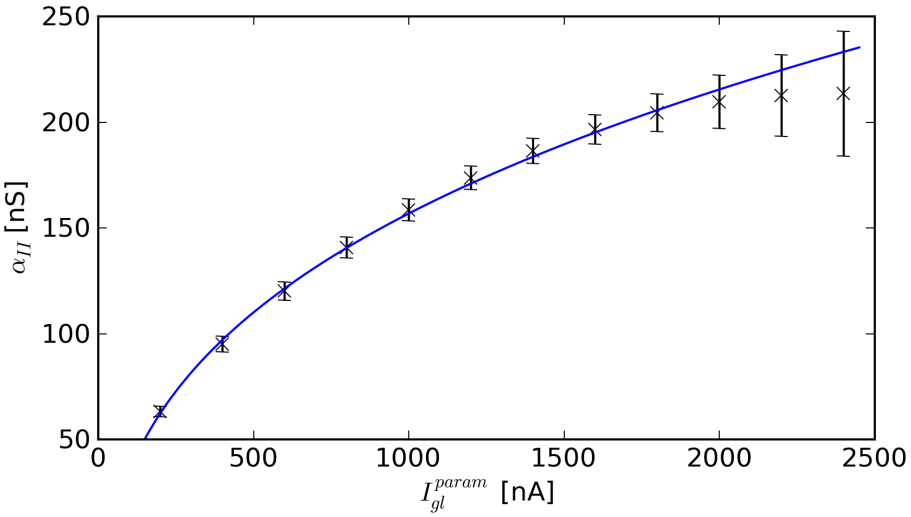

Figure 13: Differential conductance α_{II} at the OTA's saturation regime as a function of the control current. The parameterization of the blue line is listed in table 4.

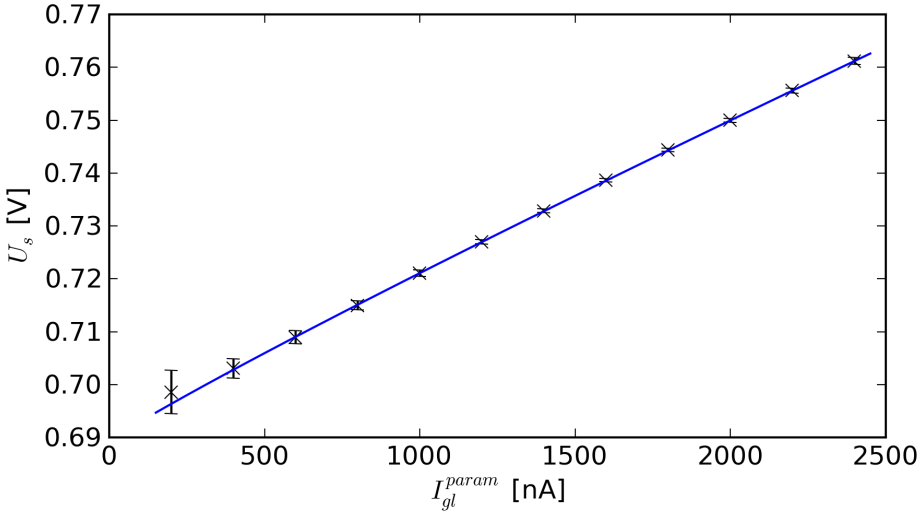

Figure 14: Saturation voltage as a function of the control current. The parameterization of the blue line is listed in table 4.

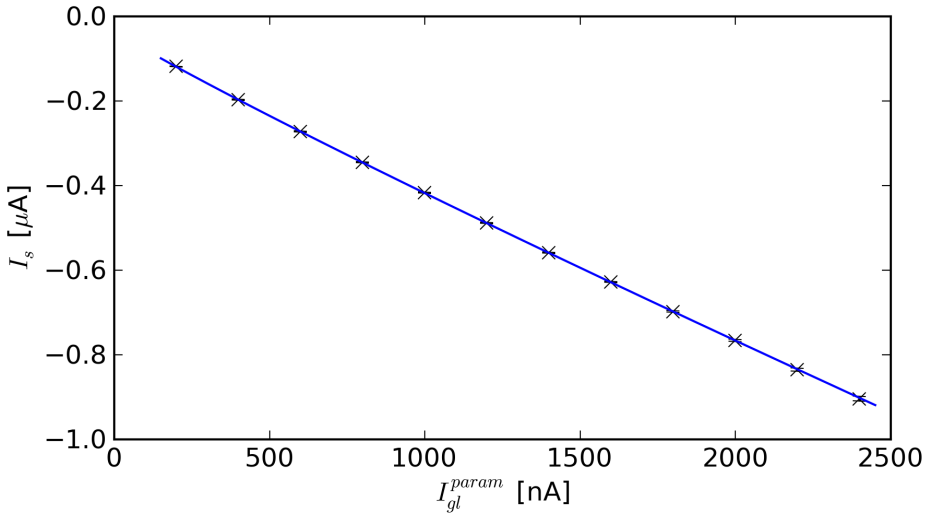

Figure 15: Saturation current as a function of the control current. The parameterization of the blue line is listed in table 4.

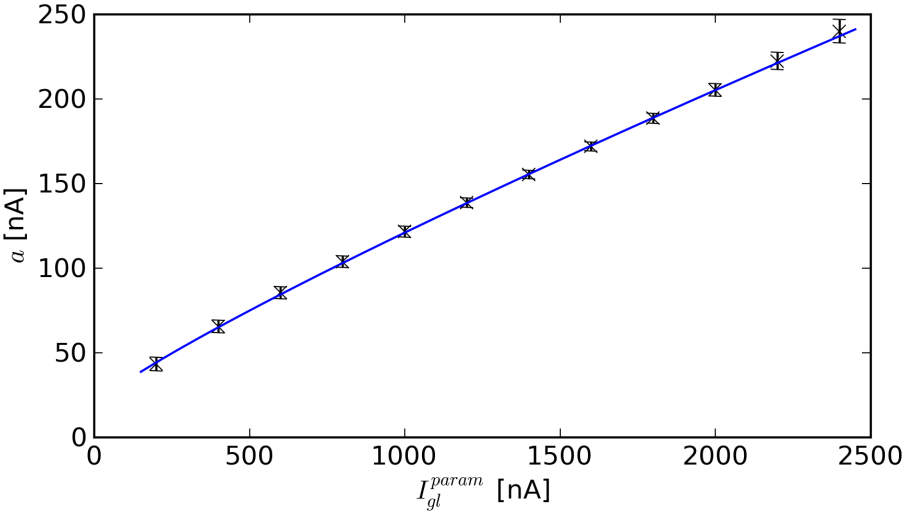

Figure 16: Transition width as a function of the control current. The parameterization of the blue line is listed in table 4.

D. Exponential Term Parameter Sets

I_bexp [nA]	**V_bexp [nA]**	**I_rexp [nA]**	**V_exp [mV]**	**current [nA]**	**buffer voltage [mV]**	**membrane voltage [mV]**
2500	0	2500	1800	0.00 ± 0.03	1547	597
2500	0	100	1800	0.00 ± 0.03	1547	597
2500	0	100	$600 = E_l$	0.00 ± 0.03	600	597
0	0	100	200	0.00 ± 0.03	205	597
0	0	2500	0	0.00 ± 0.03	76	597
2500	2500	2500	1500	0.00 ± 0.03	601	599
2500	2500	100	1500	0.00 ± 0.03	601	599
2500	2500	100	$600 = E_l$	0.00 ± 0.03	601	599
0	2500	100	200	39.3	950	604
0	2500	2500	0	637.8	1144	681
0	2500	750	536	637.8	1144	681

Table 5: Tested configurations of the exponential term. The measures are taken in the neuron's equilibrium state. The column 'current' lists the currents running off the cell membrane. The 'buffer voltage' is the voltage controlled by the input buffer of V_{exp}. It is supposed to be equal to V_{exp}. A description of the parameters, especially for V_{bexp} and I_{bexp}, is given below.

I_{bexp} Control current to switch the operational amplifier that drives the exponential current on or off. The OP is enabled with $I_{bexp} = 2500\,\text{nA}$ and disabled with $I_{bexp} = 0\,\text{nA}$.

V_{bexp} Control current to switch the input buffer of the voltage V_{exp} on or off. The input buffer is enabled with $V_{bexp} = 0\,\text{nA}$ and disabled with $V_{bexp} = 2500\,\text{nA}$.

I_{rexp} Current to control the feedback resistor that sets the strength of the exponential rise.

V_{exp} Threshold voltage at which the exponential rise of the current starts.

E. Hardware Neuron Curve Fits

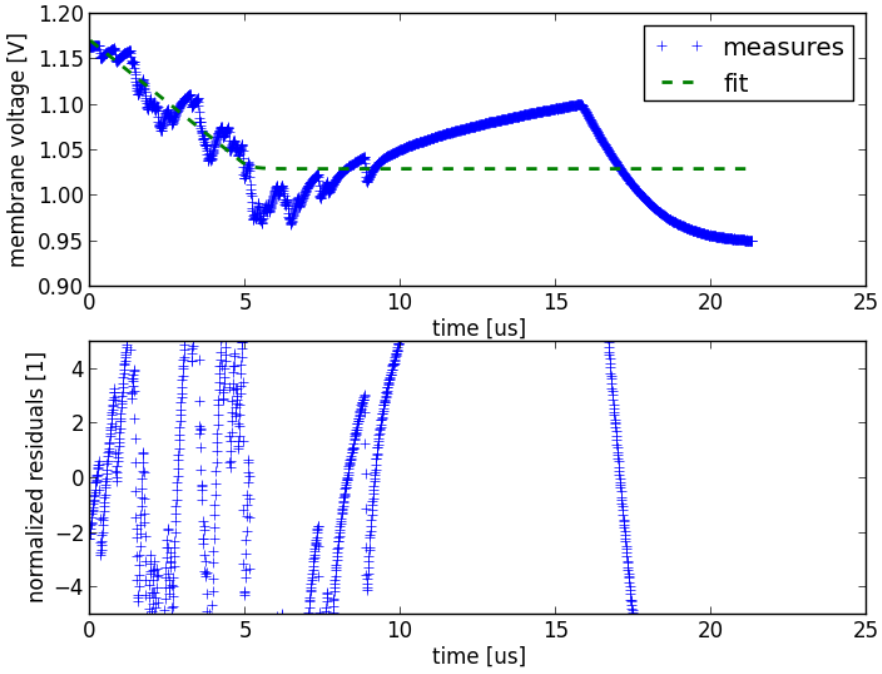

Figure 17: The membrane voltage and the curve fit of a bad neuron.

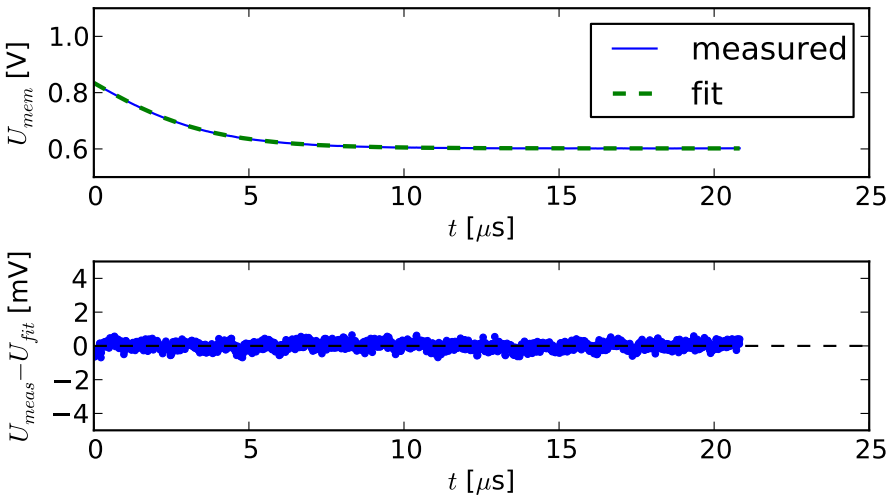

Figure 18: Membrane voltage of neuron 157. This is a typical graph of the curve fit. The noise is spread symmetric.

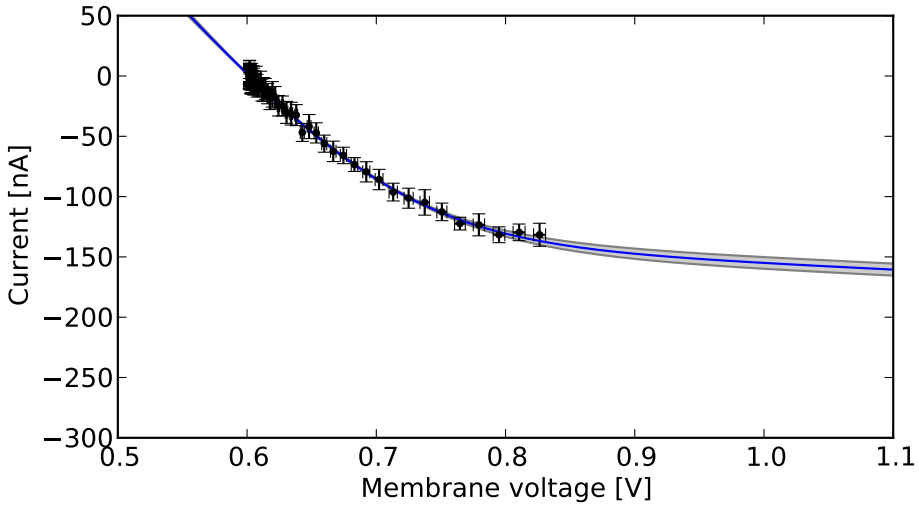

Figure 19: The $I(U)$ characteristic extracted from the data sample shown in figure 18.

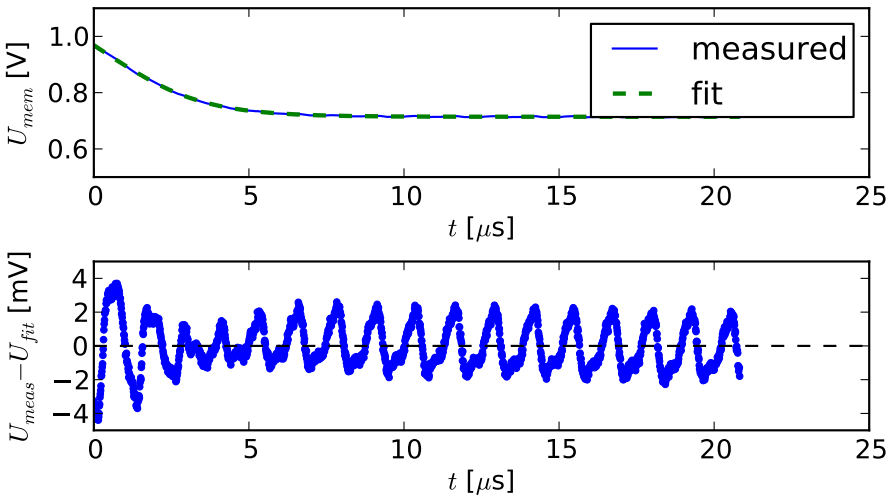

Figure 20: Membrane voltage of neuron 72. Another type of typical graph of the curve fit. The noise is spread periodically symmetric.

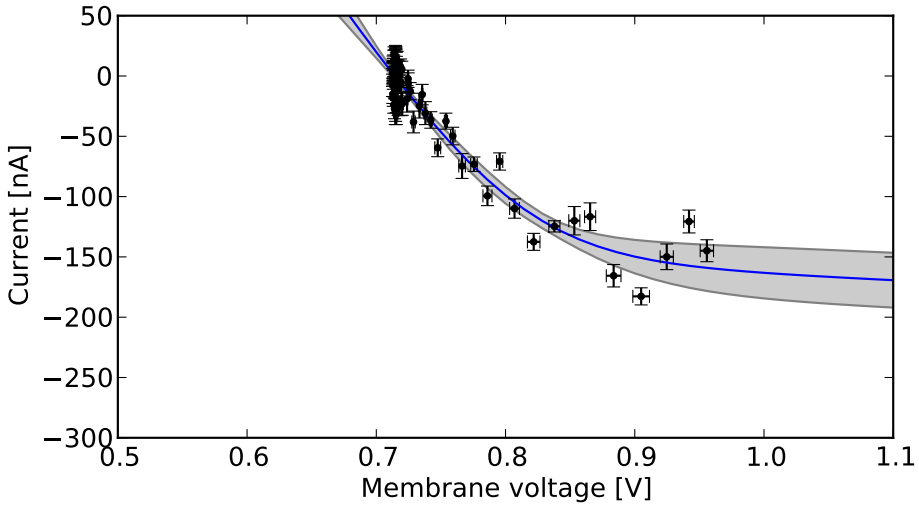

Figure 21: The $I(U)$ characteristic extracted from the data sample shown in figure 20.

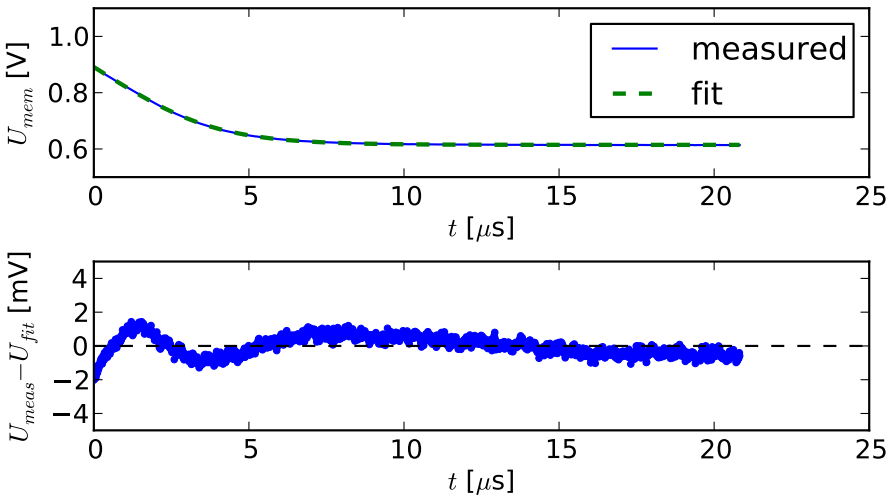

Figure 22: Membrane voltage of neuron 429. The curve fit shows a systematic error.

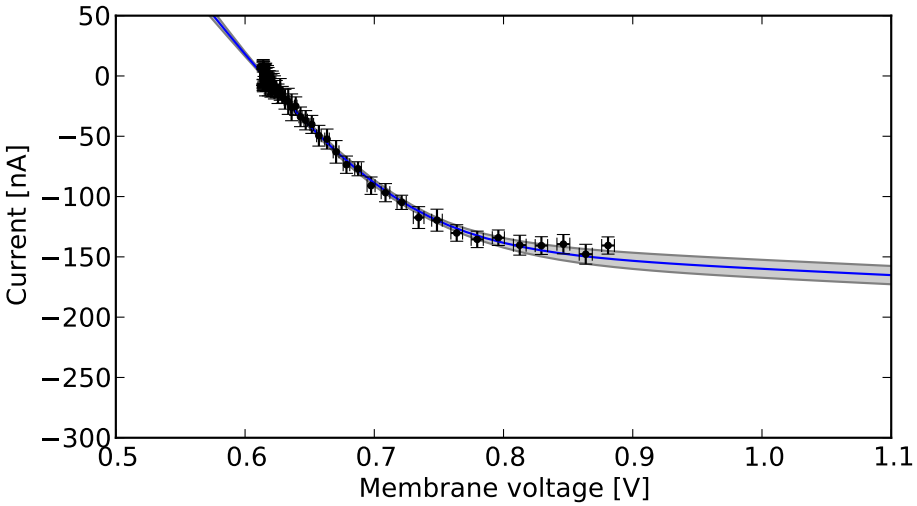

Figure 23: The $I(U)$ characteristic extracted from the data sample shown in figure 22.

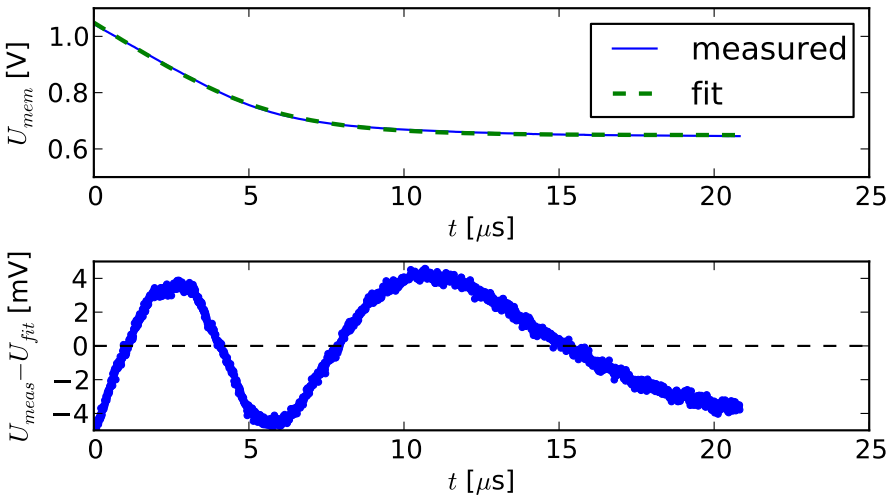

Figure 24: Membrane voltage of neuron 453. The curve fit for this neuron shows the worst systematic error.

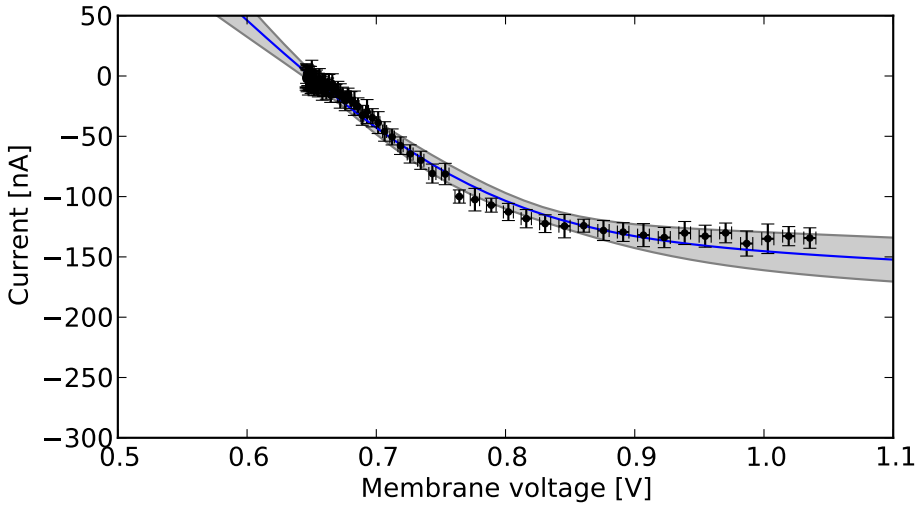

Figure 25: The $I(U)$ characteristic extracted from the data sample shown in figure 24.